Crystal structure from one-electron theory

Hans L. Skriver
Risø National Laboratory, DK-4000 Roskilde, Denmark
(Received 3 October 1984)

We have studied the crystal structures of all the $3d$, $4d$, and $5d$ transition metals at zero pressure and temperature by means of the linear muffin-tin orbital method and Andersen's force theorem. We find that, although the structural energy differences seem to be overestimated by the theory, the predicted crystal structures are in accord with experiment in all cases except $_{79}$Au. In addition, we have investigated the effect of pressure upon the alkali metals ($_3$Li, $_{11}$Na, $_{37}$Rb, $_{55}$Cs) and selected lanthanide metals ($_{57}$La, $_{58}$Ce, $_{71}$Lu) and actinide metals ($_{90}$Th, $_{91}$Pa). In these cases the theory gives accurate predictions of the stability of the close-packed structures but is found to be less accurate for open structures such as α-U.

I. INTRODUCTION

The crystal structures of elemental metals tend to occur in certain sequences when viewed as functions of atomic number or hydrostatic pressure. The most prominent example of this phenomenon is the d transition metals, where all three transition series, excluding the four magnetic $3d$ metals, exhibit the same hcp→bcc→hcp→fcc sequence as the d bands become progressively filled (Fig. 1). Qualitative explanations of this trend have been given by Brewer[1] in terms of Engel correlations between the valence sp electrons, and by Kaufman and Bernstein[2] in terms of semiempirical thermodynamic calculations of phase diagrams, whereas Deegan,[3] Dalton and Deegan,[4] and Ducastelle and Cyrot-Lackmann[5] have attempted more quantitative approaches based on one-electron theory.

Dalton and Deegan[3,4] showed that the stability of the bcc phase for nearly-half-filled d shells might be explained by differences in the sum of one-electron band-structure energies, and they pointed to the special double-peak structure of a bcc state density as being responsible for this stability. Later, Pettifor[6,7] extended the work of Dalton and Deegan and showed that the entire crystal-structure sequence of the transition metals could be accounted for by a one-electron approach. In his calculations, Pettifor[8] found no evidence for the Brewer-Engel correlation,[1] which relates crystal-structure stability to the sp-occupation numbers, and instead he related the hcp→bcc→hcp→fcc sequence to the change in d occupation which takes place across a transition series. This latter viewpoint has proven to be very fruitful in that it may be used as a simple "one-parameter theory," which, in many cases, provides remarkably good estimates of

0.0 - 0.8											
Li hcp	Be hcp										
Na hcp	Mg hcp	1	2	3.5	5	6	7	8.5	9.5	10	n_d
K bcc	Ca fcc	Sc hcp	Ti hcp	V bcc	Cr bcc	Mn (bcc)	Fe bcc	Co hcp	Ni fcc	Cu fcc	Zn hcp
Rb bcc	Sr fcc	Y hcp	Zr hcp	Nb bcc	Mo bcc	Tc hcp	Ru hcp	Rh fcc	Pd fcc	Ag fcc	Cd hcp
Cs bcc	Ba bcc	Lu hcp	Hf hcp	Ta bcc	W bcc	Re hcp	Os hcp	Ir fcc	Pt fcc	Au fcc	Hg (fcc)
Fr	Ra bcc										

La dhcp	Ce fcc	Pr dhcp	Nd dhcp	Pm dhcp	Sm Sm-t	Eu bcc	Gd hcp	Tb hcp	Dy hcp	Ho hcp	Er hcp	Tm hcp	Yb hcp
Th fcc	Pa bct	U orth.	Np orth.	Pu mon.	Am dhcp	Cm dhcp	Bk dhcp	Cf dhcp	Es	Fm	Md	No	Lr

FIG. 1. Crystal structures of the metallic elements at low temperature.

structural stabilities also for nontransition metals, such as the alkaline earths.[9]

The crystal structures of the trivalent lanthanides, i.e., $_{59}$Pr through $_{71}$Lu, except for $_{63}$Eu and $_{70}$Yb, exhibit such regularity, as functions of atomic number, pressure, and temperature, that Johansson and Rosengren[10] were able to construct a single generalized phase diagram for these metals. In this case the crystal structures observed under ambient conditions[11] are found to be part of the sequence hcp→Sm-type→dhcp→fcc→fcc′ established by high-pressure experiments[12–19] and alloying.[20] Here fcc′ refers to the recently discovered distorted fcc structure.[21] The lanthanide sequence is also found in $_{39}$Y (Ref. 22), where there are no occupied f states, and in the heavier actinides,[23–28] at pressures where the $5f$ states are still localized. Qualitative explanations of the hcp→Sm-type →dhcp→fcc sequence have been attempted in terms of pseudopotential theory by Hodges,[29] and in terms of a $4f$ contribution to the bonding by Gschneidner and Valletta,[30] while Duthie and Pettifor[31] gave a quantitative explanation in terms of one-electron theory.

Duthie and Pettifor[31] showed that the lanthanide crystal-structure sequence could be explained by differences in the total one-electron band-structure energies, and they found a strong correlation between crystal structure and d-occupation number. Hence it appears that the lanthanide metals, as far as their crystal structures are concerned, behave as ordinary $5d$ transition metals with a d occupation ranging from approximately 2.0 in $_{57}$La to 1.5 in $_{71}$Lu. This result is very appealing because there is a one-to-one correspondence between the calculated d-occupation number and the single f parameter used by Johansson and Rosengren[10,32] to rationalize the lanthanide crystal-structure sequence, and because it is immediately possible to understand the behavior[22] of $_{39}$Y and the heavy actinides[23–28] within the same framework.

It may at first sight seem surprising that the crystal structures of so many metals can be explained on the basis of differences in the total one-electron band-structure energies alone, since the total electronic energy, apart from the one-electron term, also has contributions from double counting and from exchange and correlation. However, it has recently been shown[33,34] that, provided the one-electron *potential* is kept frozen upon a displacement of the atoms, the corresponding changes in the double-counting and exchange-correlation terms cancel[35] to first order in the appropriate local electron density, and hence the difference in the sum of the one-electron energies, obtained by means of the frozen, i.e., not self-consistently relaxed, potential, will give an accurate estimate of the corresponding self-consistent change in the total electronic energy. It is exactly this cancellation, which also leads to the Hodges-Nieminen-Pettifor[36,37] pressure expression, and to the more general force relation derived by Andersen,[33] that, in turn, justifies the simple band-structure approach taken, for instance, by Pettifor.[6–8]

In their work, Pettifor[6–8] and Duthie and Pettifor[31] focused their attention on the contribution to the total energy from the d bands and either neglected hybridization with the sp bands entirely or included hybridization appropriate to some average element. Hence their picture is essentially a canonical[38] one, in which the energy-band structures depend only on crystal structure and not on band filling. It is obvious that such a picture, although adequate for the d transition metals, will fail in cases where states of non-d character are equally or more important, as they are, for instance, in the alkali, the alkaline-earth, and light actinide metals. Fortunately, the force theorem is not restricted to the canonical approximation and it has recently been used in theoretical investigations of crystal structures in the third-row metals[39,40] the alkaline-earth metals,[9] and in $_{55}$Cs above the s-d transition.[41]

In the present work we go beyond the canonical approximation and use the force theorem[33] to calculate the structural energy differences for all the $3d$ $4d$, and $5d$ transition metals at zero pressure and temperature. In addition, we investigate the effect of hydrostatic pressure on the crystal structures of alkali, alkaline-earth, lanthanide, and actinide metals.

Traditionally, the nontransition metals, e.g., alkali and alkaline-earth metals, have been treated by means of pseudopotential theory, and the crystal structures predicted from this approach are generally in good agreement with experiment.[42–47] It has, however, not been straightforward to generalize the pseudopotential method to treat narrow-d-band materials, and to do so one has had to add localized orbitals to the plane-wave basis set.[48] Thus the d band in $_{19}$K is described by the d component of plane waves, while that of $_{29}$Cu is described by additional d orbitals, which is somewhat inconsistent with the smooth lowering of the $3d$ band through the series $_{19}$K, $_{20}$Ca, $_{21}$Sc, . . . , $_{29}$Cu. The method has, however, proved to be very accurate.

The present approach, based upon the linear muffin-tin orbital (LMTO) method,[49] has the advantage of employing the same type of basis functions for all the elements, thus leading to a conceptually consistent description of trends throughout the Periodic Table. In addition, the LMTO method is extremely efficient on a computer, requiring only the solution of an eigenvalue problem of 9×9 (or 16×16 if f states are included) per atom at each point in reciprocal space. Since we are mainly interested in trends, we have neglected the nonspherical contributions to the charge density, which may explain what seems to be a systematic overestimate of the calculated structural energy differences. We have, furthermore, neglected a structure-dependent electrostatic interaction between atomic spheres, except in the few cases where it contributes significantly to the energy differences.

II. ONE-ELECTRON THEORY OF STRUCTURAL STABILITY

At low temperature the crystal structure of a metal is determined by the total electronic energy U, in addition to a small contribution from the zero-point motion[50] which we shall neglect. Hence, if one wants to determine the stability of some crystal structure, say bcc, against some reference structure, which we shall take to be the close-packed fcc structure, one may calculate the total energy of both phases and form the structural energy difference

$$\Delta_{\text{bcc-fcc}} = U_{\text{bcc}} - U_{\text{fcc}} , \quad (1)$$

where the total energy according to the local-density approximation[51] may be written as the sum over occupied states of the one-electron energies ε_i corrected for double counting, plus electrostatic terms,[52] i.e.,

$$U = \sum_i^{\text{occ}} \varepsilon_i - E_{\text{double counting}} + E_{\text{electrostatic}} . \quad (2)$$

If the difference (1) is negative, the bcc structure will be stable against fcc.

Total energies for, say, a $4d$ metal, are of the order of 10^4 Ry, mainly because of the contributions from the low-lying core levels, while typical structural energy differences are of the order of 10^{-3} Ry. Hence, extreme accuracy is needed in order to use (1) directly, and one would like to have a numerically more satisfactory procedure. The force theorem[33] gives rise to such a procedure, but, more importantly, perhaps it casts the problem of finding stable crystal structures into a form where the significant contribution comes from the one-electron valence energies and neither from double counting, nor from the deep core levels.

The force theorem dictates the following procedure. For a given metal at a given atomic volume one must solve the energy-band problem self-consistently, assuming the reference crystal structure. To this end we use the LMTO method[49] within the atomic-sphere approximation (ASA), including the combined correction to the ASA.[49] In addition, we take into account the relativistic effects, except for spin-orbit coupling, which we neglect, include exchange-correlation in the form given by von Barth and Hedin,[53] and freeze the appropriate cores. This part of the calculations is described in detail by Skriver.[54] We have now minimized the energy functional $U\{n\}$ with respect to changes in the electron density n, and obtained the ground-state density $n^{\text{SC}}_{\text{fcc}}$. Because of the stationary properties of U, one may obtain, for instance, U_{bcc} from a trial charge density $n^{\text{tr}}_{\text{bcc}}$ constructed by positioning the self-consistent fcc atomic-sphere *potentials* in a bcc geometry, solving the one-electron Schrödinger equation, and populating the lowest-lying one-electron states. Hence,

$$\Delta_{\text{bcc-fcc}} = U_{\text{bcc}}\{n^{\text{tr}}_{\text{bcc}}\} - U_{\text{fcc}}\{n^{\text{SC}}_{\text{bcc}}\} , \quad (3)$$

where the errors relative to (1) are of second order in $n^{\text{tr}}_{\text{bcc}} - n^{\text{SC}}_{\text{bcc}}$. Now, the use of a *frozen*, i.e., not self-consistently relaxed, *potential*, to generate $n^{\text{tr}}_{\text{bcc}}$ ensures that the chemical shifts in the core levels drop out of Eq. (3), and also that the double-counting terms cancel. Hence, the core-level energies and the double-counting terms may be neglected entirely in Eq. (2), leaving only the valence one-electron energies and the electrostatic terms to be considered. The fact that the freezing of the potential leads to such a computationally simple and conceptually important result was already noted by Pettifor in his derivation of the pressure expression.[37]

Within the atomic-sphere approximation,[49] the atomic Wigner-Seitz sphere of an elemental metal is neutral, and there is therefore no electrostatic interaction between the spheres. Hence the electrostatic terms in Eq. (2) vanish and the structural energy difference (3) may be obtained from

$$\Delta_{\text{bcc-fcc}} = \int^{E_F} E N_{\text{bcc}}(E) dE - \int^{E_F} E N_{\text{fcc}}(E) dE , \quad (4)$$

where $N(E)$ is the one-electron state density. Furthermore, the ASA allows a separation of the potential- and crystal-structure-dependent parts of the energy-band problem.[38,49,54] Hence, all that is required at a given atomic volume, in addition to the self-consistent fcc calculation, is to calculate the energy bands of the relevant crystal structures with the use of the self-consistent fcc potential parameters, evaluate the sums of the one-electron energies, and subtract according to Eq. (4). This procedure is quite general, treats all s, p, d, and f electrons on the same footing, and may be applied to all metals in the Periodic Table.

III. MADELUNG CORRECTION TO THE ASA

The errors of neglecting the struture-dependent electrostatic terms in (2) may be estimated by means of what has been called either the muffin-tin[55] or Ewald[56] correction to the ASA. To derive this correction, one observes that the electrostatic energy per ion of a lattice of point ions of charge $q_s \mid e \mid$ embedded in a negative neutralizing uniform charge density is given by the well-known Madelung expression

$$U_M = -\tfrac{1}{2}(q_s \mid e \mid)^2 \frac{\alpha_M}{S} , \quad (5)$$

where α_M is the lattice Madelung constant and S is the atomic Wigner-Seitz radius. In the ASA this expression is approximated by the energy of an ion embedded in a single neutralizing atomic sphere, whereby $\alpha_M(\text{ASA}) = 1.8$. The correction is therefore

$$\Delta U_M = \tfrac{1}{2}(q_s \mid e \mid)^2 \frac{1.8 - \alpha_M}{S} . \quad (6)$$

In a muffin-tin model the effective charge $q_s \mid e \mid$ is the charge density in the interstitial region between the muffin-tin spheres multiplied by the volume of the unit cell. In the ASA this becomes

$$q_s \mid e \mid = \tfrac{4}{3}\pi S^3 n(S) \mid e \mid , \quad (7)$$

where $n(S)$ is the electron density at the atomic radius.

For close-packed crystal structures, α_M is approximately 1.8 (see Table I), and hence the correction (6) is smallest

TABLE I. Madelung constant to be used in Eq. (6).

i	α_M	$1.8-\alpha_M$ ($\times 10^{+3}$)	$(1.8-\alpha_M)_i-(1.8-\alpha_M)_{\text{fcc}}$ ($\times 10^{+3}$)
fcc	1.791 747 23	8.253	
bcc	1.791 858 51	8.142	−0.111
hcp	1.791 676 24	8.324	0.071
α-U[a]	1.784 182 98	15.817	7.564

[a] $b/a = 1.964$, $c/a = 1.709$, and $y = 0.1$.

in these. Typically, q_s/S lies in the range from 0.5 to 5 a.u., so that the Madelung correction for the bcc and hcp structures relative to the fcc structure lies in the range 0.05—0.5 mRy.

IV. STRUCTURAL STABILITY FROM CANONICAL BAND THEORY

In order to make contact with previous calculations,[6–8,31] we shall here briefly state the results of canonical band theory.[38,49] According to this, an unhybridized, pure l band may be obtained from[38,54]

$$E_{li}(\mathbf{k})=C_l+\frac{1}{\mu_l S^2}\frac{\mathscr{S}_{li}^{\mathbf{k}}}{1-\gamma_l\mathscr{S}_{li}^{\mathbf{k}}}\ , \tag{8}$$

where the $\mathscr{S}_{li}^{\mathbf{k}}$ are the canonical bands, which depend solely on the crystal structure, S is the atomic Wigner-Seitz radius, C_l is the center of the l band, μ_l is the band mass, and γ_l is a distortion parameter. The three potential parameters C_l, μ_l, and γ_l depend on potential and volume, but not on crystal structure.

In a transition metal one may, to a good approximation, neglect all but the d bands. Since, furthermore, γ_d is small, one has the following potential-, i.e., atomic-number-, independent estimate of the band contribution to the cohesive energy E_c,

$$\begin{aligned}\mu_d S^2 E_c &= -\mu_d S^2\int^{E_F}(E-C_d)N_d(E)dE\\ &= -\int^{\mathscr{S}_d(n_d)}\mathscr{S}_d\tilde{N}_d(\mathscr{S}_d)d\mathscr{S}_d\ ,\end{aligned} \tag{9}$$

in terms of the first-order moment of the canonical state density $\tilde{N}_d$. Andersen *et al.*[57] have evaluated (9) as a function of d-occupation number n_d and found the expected parabolic behavior,[58] which may also be obtained directly if $N_d(E)$ is approximated by a rectangular state density.

Since the center C_d and the band mass μ_d are independent of crystal structure, the first-order moment (9) may be used to estimate the structural energy differences according to Eq. (4). The result shown in Fig. 2 is identical to that of Andersen *et al.*,[57] and similar to that obtained by Pettifor.[6] It accounts qualitatively for the crystal structures of the nonmagnetic transition metals (Fig. 1) in the beginning of the series, but fails to predict the fcc structure at high d occupations. This failure is attributed either to a failure of the force relation[33] or to hard-core effects[6–8] not included in Eq. (9).

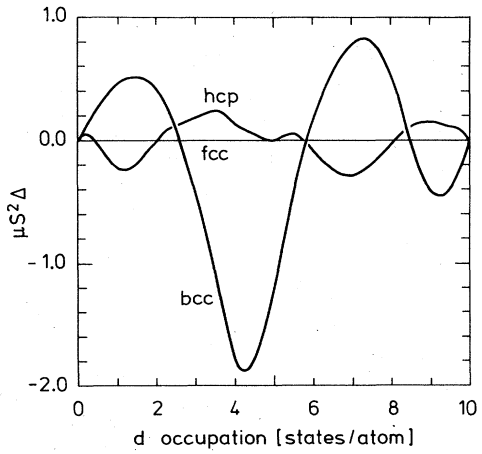

FIG. 2. Structural energy differences obtained from canonical d bands, by means of Eq. (4), as functions of the calculated canonical d occupation.

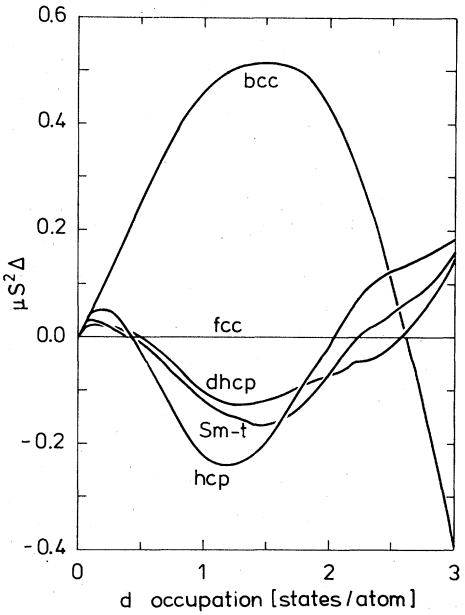

FIG. 3. Structural energy differences obtained from canonical d bands, by means of Eq. (4), in the d-occupation-number range appropriate to the lanthanide crystal-structure sequence.

The lanthanide metals are found to have d-occupation numbers varying almost linearly with atomic number from 1.99 in $_{57}$La to 1.45 in $_{71}$Lu (Ref. 59), or from 2.5 to 2.0 if hybridization is neglected.[31] Furthermore, their crystal structures are as closely packed as those of the d transition metals, and hence their structural energy differences may be estimated by Eq. (9). The results shown in Fig. 3 are qualitatively similar to, but, on the average, a factor of 1.7 smaller than, those obtained by Duthie and Pettifor.[31] In this comparison one may take the d-band width to be approximately $25/\mu_d S^2$ in order to bring their Fig. 2 onto the scale of our Fig. 3. The results in Fig. 3 account qualitatively for the hcp→Sm-type→dhcp sequence found experimentally upon going from Lu to La, and, more importantly perhaps, since the d occupation for the lanthanides is calculated to increase with pressure and decrease with atomic number, they also explain that part of the same sequence is realized when a particular lanthanide metal is subjected to pressure. It therefore follows that the d-occupation number, which is essentially a measure of the relative position of the s and d bands, may be used to rationalize the structure of the generalized phase diagram for the lanthanides constructed by Johansson and Rosengren.[10]

At the present stage, one should realize that the results obtained by canonical band theory and shown in Figs. 2

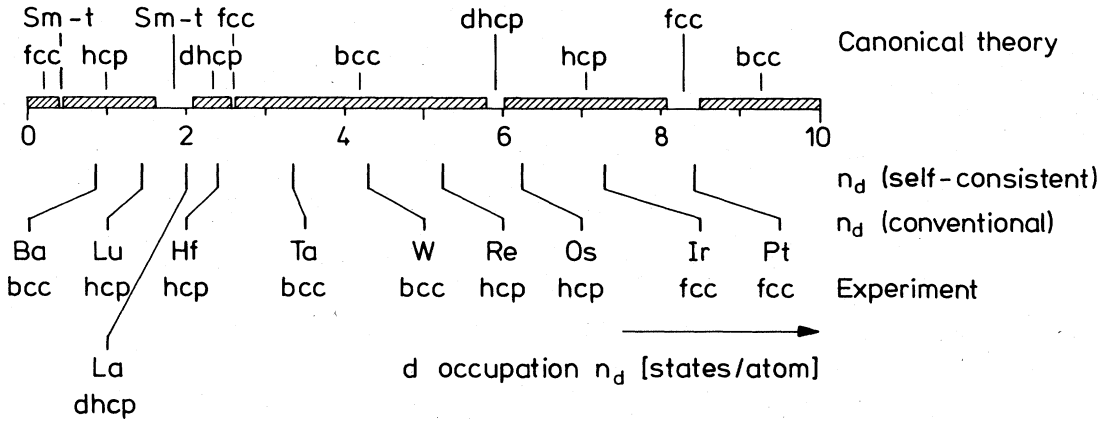

FIG. 4. Canonical estimate of the most stable close-packed crystal structure as a function of the calculated d-occupation number compiled from Figs. 2 and 3 (horizontal bars). Given below are two estimates of the actual d-occupation numbers of the $5d$ metals, together with the experimentally observed crystal structures.

and 3 are only qualitative. Indeed, if one considers Fig. 4, where the canonical estimates are compared with experimental crystal structures, one finds that the canonical theory in several cases does not predict the correct crystal structure independently of whether one uses the self-consistent d-occupation numbers or those obtained conventionally by nonlinear interpolation along a row in the Periodic Table (see Fig. 1). $_{57}$La, $_{75}$Re, and $_{77}$Ir, for instance, are examples of incorrect predictions, but here one may argue that the correct crystal structure is nearby, and hence the failure of the theory may be considered to be less important. $_{56}$Ba is another example, and in this case there is no nearby bcc structure. However, in $_{56}$Ba the d-occupation number is only a fraction of the total number of electrons, and hence a theory based solely on unhybridized d bands is probably inapplicable. The most important failure is connected with the d-occupation range from 1.6 to 2.6 states/atom. According to Fig. 4, $_{57}$La, $_{59}$Pr, $_{60}$Nd, and $_{61}$Pm should incorrectly form in the Sm-type structure, while $_{22}$Ti, $_{40}$Zr, and $_{72}$Hf are expected to be part of the lanthanide sequence. Instead, the latter three metals form in the hcp structure, which is the least stable among those considered in the d-occupation range above 2 states/atom.

It may be concluded that the simple estimate of structural energy differences obtained by means of the first-order moments of the canonical state densities is of limited value as a predictive tool. It is, however, of sufficient physical significance to warrant a study of the crystal structure of metals using a more accurate one-electron theory and to be used in the interpretation of the results of such a study.

V. STRUCTURAL STABILITY FROM LMTO BAND CALCULATIONS

In the following we shall present structural energy differences for most metallic elements to the left of and including the noble metals, as obtained by means of the procedure described in Sec. II. The results will be valid only at low temperature and at atmospheric pressure, strictly $T=0$ K and $P=0$ GPa, except in a few important cases where structural stability has been followed as a function of pressure.

A. The alkali metals

The calculated structural energy differences for alkali metals at equilibrium are almost 2 orders of magnitude smaller than those of, for instance, the alkaline-earth metals. To judge the accuracy of our approach, we have therefore studied these differences as functions of pressure, as shown in Fig. 5, from equilibrium down to a compression of 2.5. The results in Fig. 5 include the Madelung correction (6), which turns out to be crucial in the comparison with recent pseudopotential and LMTO results.[39,40,45]

From Fig. 5 it is expected that the heavy alkali metals

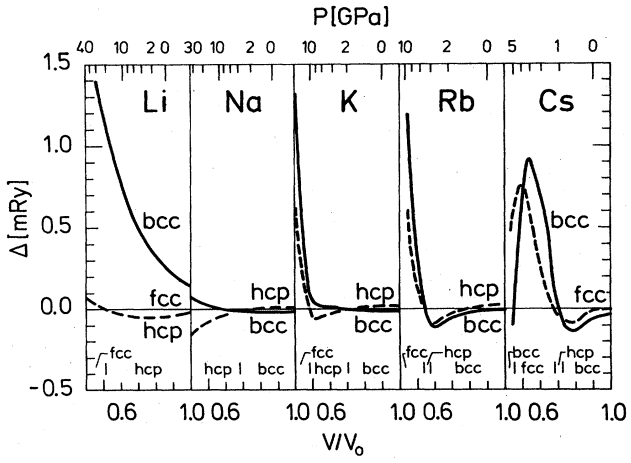

FIG. 5. Structural energy differences for the five alkali metals as functions of the relative volume V/V_0. At the top is given the calculated LMTO pressure P. The calculations included s, p, and d orbitals and the Madelung correction, Eq. (6).

at low temperature and pressure should form in the bcc structure, while Li should be hcp. Experimentally, it is known[60] that all five alkali metals at room temperature form in the bcc structure, and that they remain in this structure down to 5 K, except for $_{11}$Na, which below 51 K transforms into the hcp structure, and $_{3}$Li, which at low temperature exhibits both an hcp and fcc phase. Hence, except for Na, the low-pressure structures are correctly predicted.

Recently, Moriarty[45] successfully estimated the structural stability for some 20 nontransition metals by means of his generalized pseudopotential theory (GPT). He found incorrectly (see his Table VIII) that all the alkali metals at $T=0$ K and $P=0$ GPa should form in the hcp structure, but pointed out that at a slight compression the experimentally observed bcc structure would be stable in the heavy alkali metals, $_{19}$K, $_{37}$Rb, and $_{55}$Cs. A similar problem is encountered in another recent pseudopotential study,[47] in which the structures of $_{3}$Li and $_{19}$K at low temperature and pressure are predicted in agreement with experiment, but where $_{11}$Na is expected to be fcc. On the other hand, in view of the extremely small energies involved (see Fig. 5), it is not surprising that the prediction of the low-pressure part of the alkali-metal phase diagrams is a severe test of any calculation.

In their work on the third-row metals, McMahan and Moriarty[40] compared structural energy differences obtained by means of the LMTO and GPT methods and found excellent qualitative agreement, except for $_{11}$Na. If we compare our Na results in Fig. 5 with their Fig. 1, we find, somewhat surprisingly, that our calculations are in closer agreement with their GPT than with their LMTO results. There are several reasons for the differences between the two LMTO calculations. Firstly, we have included the Madelung correction (6), without which the calculated bcc curve is entirely above, and the hcp curve entirely below, the fcc, in qualitative agreement with their LMTO results. Secondly, we have sampled the Brillouin zone on a finer mesh, i.e., 916, 819, and 448 **k** points in the irreducible wedge for fcc, bcc, and hcp, respectively, and, finally, we have improved the convergence of the reciprocal-lattice sums in the expression for the combined-correction terms,[49] whereby the numerical errors in the structural energy differences for Na are below 0.01 mRy. As a result, it appears that in the case of closely packed crystal structures the LMTO method, including the Madelung correction (6), has an accuracy comparable to that attained by pseudopotential theory.

Owing to the fact that we have only included three crystal structures in Fig. 5, $_{55}$Cs is incorrectly calculated to transform into the bcc structure at a compression of 2.2. However, in a recent study of Cs above the *s-d* transition, i.e, beyond the pressure range of the present work, McMahan[41] found that, before the bcc structure became more stable than fcc, Cs had transformed into the Cs IV structure, in agreement with high-pressure experiments.[61,62]

B. The alkali metals at moderate compression

According to Fig. 5, all the alkali metals should, at low temperature, be part of the same crystal-structure sequence, bcc→hcp→fcc, and one would anticipate that these transitions are driven by the pressure-induced lowering of initially unoccupied *d* states through the Fermi level, whereby electrons are gradually transferred from the *s* into the *d* band. If one plots the calculated crystal structures as functions of *d*-occupation number, as in Fig. 6, it is seen that only in the heavy alkali metals $_{19}$K, $_{37}$Rb, and $_{55}$Cs is this mechanism at work, while the transitions in $_{3}$Li and $_{11}$Na, at least below 35 GPa, have a different origin.

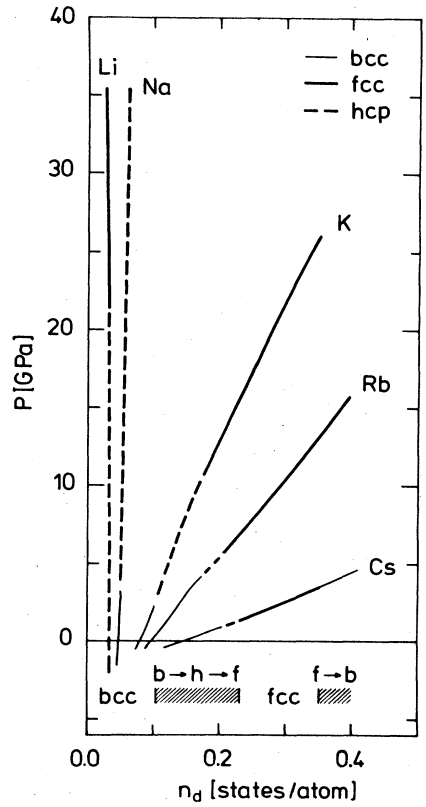

FIG. 6. Calculated crystal structures for the alkali metals as functions of the LMTO pressure and *d*-occupation number.

The experimental situation at room temperature may be summarized as followed.[63,64] Li exhibits a bcc→fcc transition at 6.9 GPa,[65] while Na remains in the bcc structure up to at least 30 GPa,[66] which substantiates the notion that the *s-d* transition is unimportant in these two metals. The heavy alkali metals all exhibit a bcc→fcc transition [$_{19}$K (Refs. 63 and 64), $_{37}$Rb (Ref. 67), $_{55}$Cs (Ref. 68)] before they transform into more complex structures, of which only the so-called Cs IV has been solved[62] so far.

There are, to our knowledge, no low-temperature high-pressure experiments which could substantiate the existence of the predicted bcc→hcp→fcc sequence, where, according to Figs. 5 and 6, the hcp phase, at least in $_{19}$K, should be stable over an appreciable pressure range. However, in view of the fact that temperature at atmospheric pressure stabilizes the bcc phase to the extent that all the alkali metals are bcc above 100 K, it is not unreasonable to assume that the intermediate hcp phase, which is only

marginally stable, is also suppressed at higher temperatures. Thus, in a high-pressure experiment at room temperature, one would see a direct bcc→fcc transition, as indeed has been observed.[63,64,67,68] If the hcp phase is suppressed, the best estimate of the room-temperature bcc→fcc transition pressure is the critical pressure for the low-temperature hcp→fcc transition (cf. Fig. 5). We find the transition pressures to be 11, 5.5, and 1.4 GPa for $_{19}$K, $_{37}$Rb, and $_{55}$Cs, respectively, which should be compared to the experimental values of 11 GPa (Ref. 64), 7 GPa (Ref. 67), and 2.2 GPa (Ref. 68).

Independent of whether the intermediate hcp phase exists or not, the high-pressure fcc phase in $_{19}$K, $_{37}$Rb, and $_{55}$Cs is much more stable than the initial bcc phase (see Fig. 5). Bardeen[69] suggested as early as 1938 that the transition observed at 2 GPa in Cs was from the normal bcc to an fcc phase, and that it resulted from the nonelectrostatic interaction energy of the ions, the important term being the Born-Mayer[70] repulsion between the ion cores. Here we shall show that the fcc phase in the heavy alkali metals owes its stability directly to the pressure-induced s-d transition, which is also shown to be the force behind, for instance, the isostructural fcc-fcc transition in Cs.[71]

In Fig. 7 we compare the important parts of the fcc and bcc band structures of Cs at the zero-pressure volume V_0 and at the volume where the fcc phase is becoming more stable than the initial bcc phase. The four band structures may be characterized as nearly-free-electron-like and s-like below the Fermi level E_F and d-like above E_F. Typical d states have symmetry labels such as Γ_{12}, $\Gamma_{25'}$, H_{12}, and X_3, and they are seen to approach the Fermi level under compression. At $V=V_0$ the fcc and bcc band structures are found to be extremely similar in that range below E_F, which is important in the sums over occupied

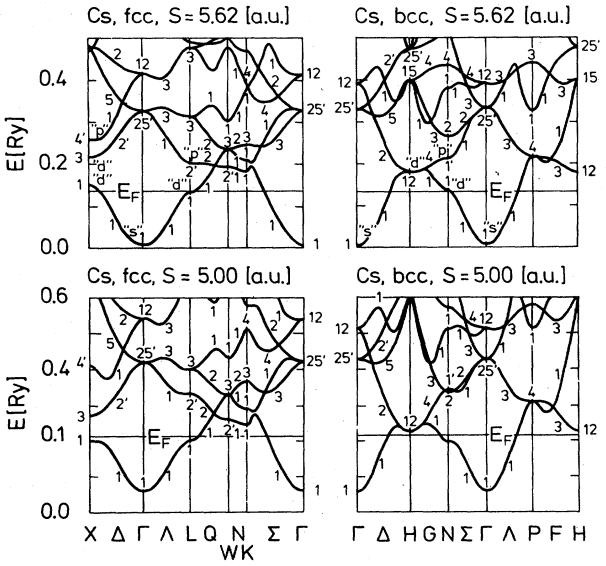

FIG. 7. Energy-band structures for Cs at equilibrium, $S=5.62$ a.u., and at a compressed volume, $S=5.00$ a.u. Conventional symmetry labels are given and the dominant s, p, or d character is indicated at a few selected energy levels.

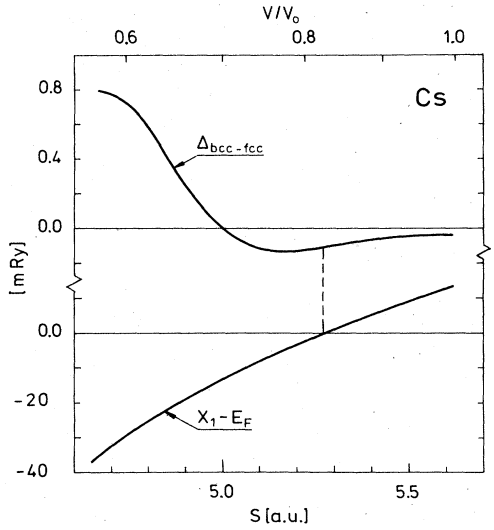

FIG. 8. Structural energy difference $\Delta_{bcc\text{-}fcc}$ for Cs (upper panel) and the position relative to the Fermi level E_F of the bottom of the gap at X in the fcc structure (lower panel) as functions of atomic radius S or relative volume V/V_0. $V=(\frac{4}{3}\pi)S^3$.

states in Eq. (4): They are both parabola shaped and "touch" E_F at a single symmetry point, L_1 for fcc and N_1 for bcc. As a result, the sums of the one-electron band-structure energies are almost equal, and the main contribution to the stability of the bcc phase comes from the electrostatic Madelung term (6), which is negative; see Table I.

At $V=0.7V_0$, hybridization with the descending d band has moved the X_1 and neighboring levels below E_F, thereby lowering the energy in the fcc phase with respect to that in the bcc phase, to the extent that the Madelung term is overcome and the structural energy difference is zero. Under further compression, the X_1 level continues to descend and the fcc phase becomes increasingly stable (see Fig. 8). This trend is eventually broken because the maximum in the $\Gamma_1\Delta_1X_1$ band moves away from X, and because the X_3 level drops below the Fermi level. Both effects destabilize the fcc structure and, subsequently, Cs transforms into the Cs IV phase. We shall not discuss this development here, but refer to the experimental work of Takemura *et al.*[62] and the theoretical treatment of McMahan.[41]

The presence of a gap at X (see Fig. 7) near the Fermi level in the compressed fcc phase, which has no counterpart in the bcc phase (nor in the hcp phase), stabilizes the fcc phase over the bcc in exactly the manner discussed by Jones in his classical work on the phase boundaries in binary alloys.[72,73] The electron states below the gap have their one-electron band energies lowered and are more densely populated than their free-electron or, here, bcc counterparts. The way the fcc phase is stabilized in Cs under pressure is shown in Fig. 8, where one notes that the stabilization occurs gradually from the point where the X_1 level crosses E_F. Hence, although the fcc phase eventually becomes more stable than the bcc phase because of the presence of the band gap at X, there is no

direct relation between the volume ($V=0.70V_0$) where the phase transition occurs and the volume ($V=0.82V_0$) where the Van Hove singularity connected with the X_1 level moves through the Fermi level. This delayed action is characteristic of many electronically driven transitions.

In the discussion of the stability of the fcc phase, we have, for simplicity, considered only Cs, but examination of the band structures for K and Rb shows that the above picture applies equally well to these two metals, although there are quantitative differences between $_{19}$K, $_{37}$Rb, and $_{55}$Cs caused by the fact that the zero-pressure position of the initially unoccupied d band drops relative to the Fermi level as the atomic number increases.

C. The alkaline-earth metals

The calculated structural energy differences for the alkaline-earth metals under pressure are shown in Fig. 9. In the figure the metals are ordered according to their calculated d-occupation number at equilibrium, and we have included the two divalent rare-earth metals $_{63}$Eu and $_{70}$Yb, but excluded the divalent metals $_4$Be and $_{12}$Mg since they do not really belong to the crystal-structure sequence we shall presently be discussing. The results at zero pressure for Be and Mg may, however, be found in the preliminary account[9] of the present work.

According to Fig. 9, $_{20}$Ca, $_{70}$Yb, and $_{38}$Sr at low temperature and pressure should form in the fcc structure, while $_{63}$Eu, $_{88}$Ra, and $_{56}$Ba should be bcc. These predictions are in agreement with experiments,[60] except for $_{70}$Yb, which, at low temperature, takes up the hcp structure.[74] However, at a slightly expanded volume the hcp phase is calculated to be the stable phase, and hence one may not have to appeal to zero-point motion to explain the anomalous low-temperature hcp phase in $_{70}$Yb. Previous pseudopotential calculations[42] have explained the bcc structure in $_{56}$Ba and the pressure- (and temperature-) induced fcc→bcc transition in $_{38}$Sr, but gave an incorrect (bcc) zero-pressure crystal structure in $_{20}$Ca. Later pseudopotential results[44] indicated that the stable structure at ordinary pressure should be the fcc structure for all the alkaline-earth metals. Hence, it is still a challenge to pseudopotential theory to predict the crystal structures of the alkaline-earth metals as a function of both atomic number and pressure.

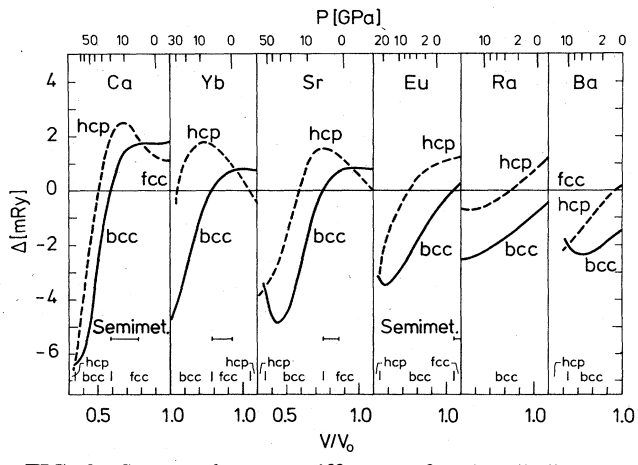

FIG. 9. Structural energy differences for the alkaline-earth metals and the two divalent rare-earth metals, Eu and Yb, as functions of relative volume V/V_0 and LMTO pressure P. The volume range over which the elements are calculated to be semimetallic is indicated by horizontal bars. The calculations included s, p, and d orbitals, but not the Madelung correction, Eq. (6).

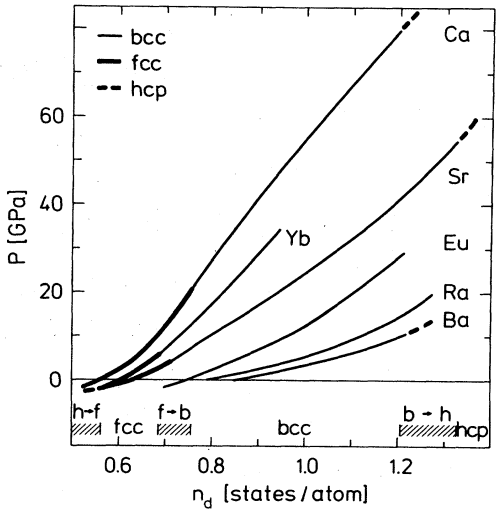

FIG. 10. Calculated crystal structures for the alkaline-earth metals as functions of the LMTO pressure and d-occupation number.

There is a strong correlation between the calculated d-occupation number and the calculated crystal structure, as may be seen in Fig. 10, according to which the heavy alkaline-earth metals should be part of the same hcp→fcc→bcc→hcp sequence. At zero pressure each individual metal may be characterized as being at different stages on the continuous s-to-d transition, i.e., by their d-occupation number, and the structural phase transitions are then driven by the pressure-induced lowering of the d band with respect to the s band. The correlation is, however, not perfect, and the calculated crystal structure changes occur over a narrow range of d-occupation numbers.

Experimentally,[75–78] one observes, at room temperature, the fcc→bcc part of the above sequence, but the bcc→hcp transition is only found in $_{56}$Ba, whereas the lighter alkaline-earth metals transform into more complex high-pressure phases[75] not considered here. The critical pressures for the fcc→bcc transition in $_{20}$Ca, $_{38}$Sr, and $_{70}$Yb, plus the bcc→hcp transition in $_{56}$Ba, are calculated to be 21, 3.8, 5.5, and 10 GPa, respectively (cf. Fig. 10). At room temperature, Olijnyk and Holzapfel[75] find, experimentally, 19.7 GPa for the transition in $_{20}$Ca, while a low-temperature extrapolation of the high-pressure crystallographic measurements by Jayaraman *et al.*[76–78] gives 4, 5, and 5 GPa for the latter three transitions. In view of the fact that no adjustable parameters have been used to construct Fig. 10, the agreement with the calculated criti-

cal pressures may be considered satisfactory.

The band-structure calculations show, in agreement with the high-pressure resistivity data,[79–82] that $_{20}$Ca, $_{38}$Sr, and $_{70}$Yb in the fcc phase should undergo a metal-semimetal-metal transition under pressure, as is described in detail for $_{20}$Ca by Jan and Skriver.[83] Recently, Dunn and Bundy[84] remeasured Ca and found the pressure range of the semimetallic phase to be much narrower than that found in earlier measurements[79] or predicted by band theory.[83,85,86] Jan and Skriver,[83] for instance, predicted that fcc Ca should be semimetallic from 4 to 29 GPa. In the present extension of those calculations, it is seen, Fig. 9, that before Ca reaches 29 GPa it is expected to transform into the bcc phase, whereby the semimetallic behavior will be terminated already at 21 GPa. This termination of the semimetallic phase at approximately 20 GPa is in agreement with both resistivity[84] and crystallographic[75] measurements. However, the critical pressure of 4 GPa for the onset of the semimetallic behavior is still too low compared to that obtained from the resistivity data,[84] and this discrepancy must be due to a failure of local-density theory of the kind mentioned in Ref. 83.

In recent high-pressure measurements,[87,88] both $_{63}$Eu and $_{70}$Yb are found to transform from the bcc to the hcp phase, in seeming agreement with the systematics exhibited in Fig. 10. However, since $_{70}$Yb,[89] and presumably also $_{63}$Eu,[10,90] are changing valence under pressure, their high-pressure hcp phase is more appropriately thought of as belonging to the rare-earth sequence (see Fig. 1), whereby it follows that $_{63}$Eu and $_{70}$Yb at very high pressure should exhibit the well-known hcp→Sm-type→dhcp→fcc transitions.

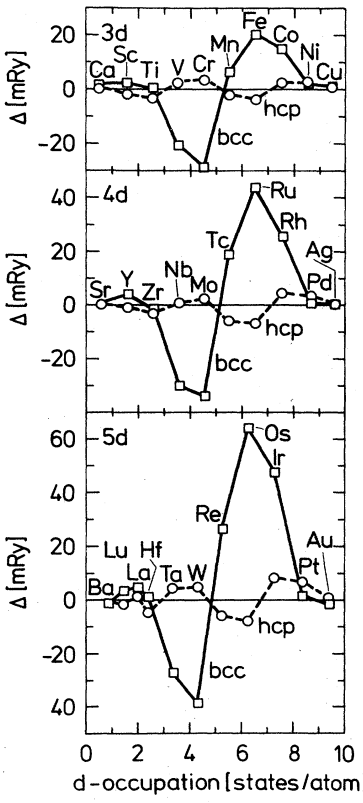

FIG. 11. Structural energy differences for the $3d$, $4d$, and $5d$ transition metals calculated at the experimentally observed equilibrium volume and plotted as functions of the d-occupation numbers. The calculations included s, p, and d orbitals, but not the Madelung correction, Eq. (6).

D. The transition metals

The calculated structural energy differences for the $3d$, $4d$, and $5d$ transition metals are shown in Fig. 11, and, as a comparison will show, the crystal structures of all the metals included in this figure, neglecting the three ferromagnetic $3d$ metals, are predicted in agreement with the experimentally observed crystal structures, Fig. 1, except for the case of Au, where the bcc structure is calculated to be marginally more stable than fcc. Hence, it follows that by including complete, i.e., fully hybridized, band structures for each individual metal, but still retaining the force theorem, one has cured most of the problems connected with the simple canonical picture discussed in Sec. IV and exemplified in Fig. 4. Furthermore, one should note that the correlation between crystal structure and d occupation, which the canonical description predicts, remains valid also for the complete calculations.

The results in Fig. 11 are very similar to those obtained by Pettifor[6–8] for the $3d$ metals and by Williams[91] for the $4d$ metals. However, despite the facts that the theoretical calculations agree within 25% and that the crystal structures of 27 metals are correctly predicted by the theory, the calculated structural energy differences are found to be as much as a factor of 3—5 larger than the enthalpy

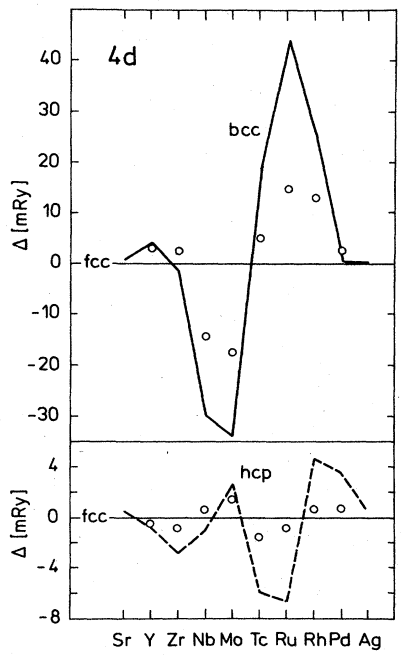

FIG. 12. Calculated (bcc)—(fcc) and (hcp)—(fcc) structural energy differences (solid and broken lines) for the $4d$ metals compared with the enthalpy differences derived from phase-diagram studies (Ref. 92) (open circles).

differences obtained from the study of binary phase diagrams,[92] Fig. 12. At present, the cause of this discrepancy is not known. The most likely candidates are either neglect of nonspherical terms in the charge density or a genuine failure of the local-density approximation. The force theorem itself does not seem to be the cause of the discrepancy, since Williams[91] obtains results similar to ours by subtraction of total-energy calculations. Finally, the "experimental" results derived by Miedema and Niessen[92] are certainly model dependent and may therefore have larger error bars.

E. The lanthanide metals

The calculated structural energy differences for the two lanthanide metals $_{57}$La and $_{71}$Lu, which bracket the lanthanide series, are shown in Fig. 13. To compare directly with the canonical results, Fig. 3, the energy differences have been brought onto the canonical scale and plotted as functions of the calculated d-occupation number. The results in Fig. 13 are qualitatively similar to the canonical results, but the energy differences are generally smaller, approximately a factor of 2, judged by, for instance, the minimum in the Sm-type curve, than their canonical counterparts. Furthermore, the lanthanide sequence has been shifted to lower d-occupation numbers, whereby the problems connected with the canonical description in the d-occupation range above 1.6 have been removed. Hence, $_{22}$Ti, $_{40}$Zr, and $_{72}$Hf are no longer part of the lanthanide sequence and are, instead, correctly predicted to form in the hcp structure, Fig. 11.

In an account of the cohesive properties of the lanthanides, Skriver[59] found that the d-occupation numbers calculated at the experimentally observed equilibrium volume decreased approximately linearly with atomic number between $_{57}$La and $_{71}$Lu. Hence, Fig. 13 may be used to estimate the equilibrium crystal structures of the lanthanide metals, excluding $_{58}$Ce because of its γ-α transition, and the two divalent metals $_{63}$Eu and $_{70}$Yb. We find, in agreement with experiments,[10] that $_{57}$La, $_{59}$Pr, $_{60}$Nd, and $_{61}$Pm should form in the dhcp structure, while $_{62}$Sm should be Sm-type. However, the heavy lanthanides are incorrectly estimated to form in the Sm-type structure. The immediate reason for this failure seems to be that the stability of the hcp structure at a given d occupation is calculated to be too low compared with dhcp and Sm-type, but the deeper cause is not known at present. As a result, the Sm-type structure extends over too wide a d-occupation range.

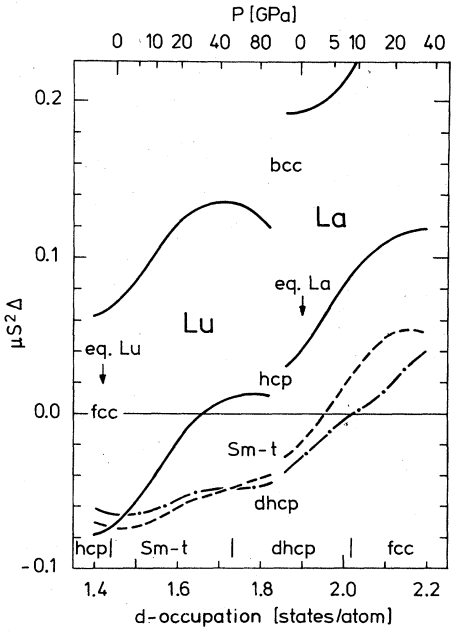

FIG. 13. Structural energy differences for La and Lu calculated as functions of pressure P and plotted vs d occupation number n_d. The calculations included s, p, d, and f orbitals, $4f$ for La and $5f$ for Lu, but not the Madelung correction, Eq. (6).

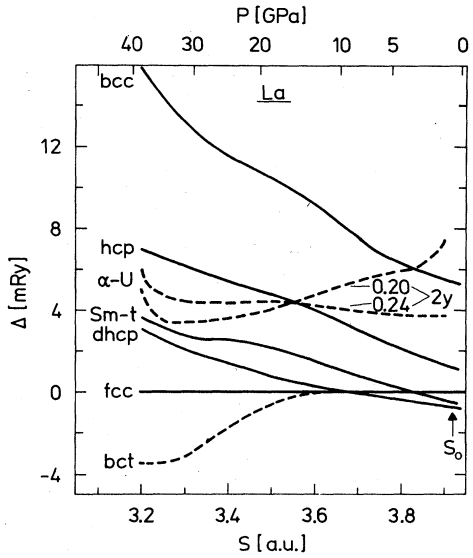

FIG. 14. Structural energy differences for La calculated as functions of pressure P and plotted versus atomic radius. The equilibrium radius $S_0 = 3.92$ a.u.

Figure 13 may also be used to predict the behavior of $_{57}$La and $_{71}$Lu under pressure. We find that Lu should transform from hcp to the Sm-type structure at -2 GPa, and into the dhcp structure at 35 GPa. Because of a 2% error in the calculated equilibrium radius, and because of the failure mentioned above, the first estimate is in error by 25 GPa, the experimental critical pressure being 23 GPa.[18] The second transition has not been observed yet. Under pressure, La is predicted to transform from dhcp to the fcc structure at 8 GPa, see also Fig. 14, which compares favorably with the experimental room-temperature transition pressure of 2.5 GPa.[13] The distorted fcc phase discovered by Grosshans *et al.*[21] has not been considered, but we shall return to the high-pressure properties of La in the following section.

F. Cerium metal under pressure

The behavior of $_{58}$Ce under pressure has been a subject of long-standing and some controversy, primarily because

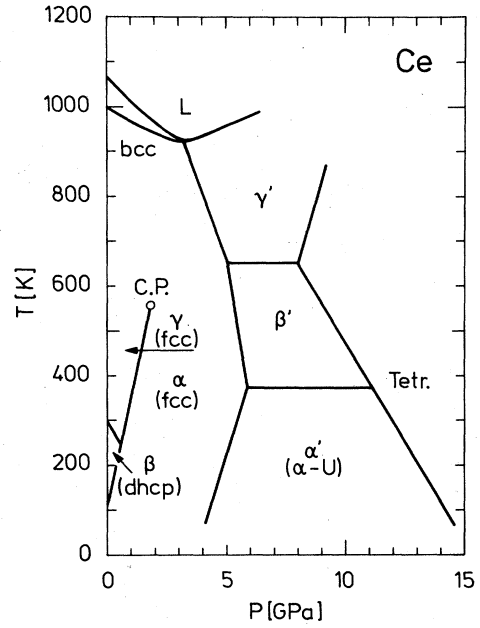

FIG. 15. Phase diagram for Ce compiled from Ref. 93.

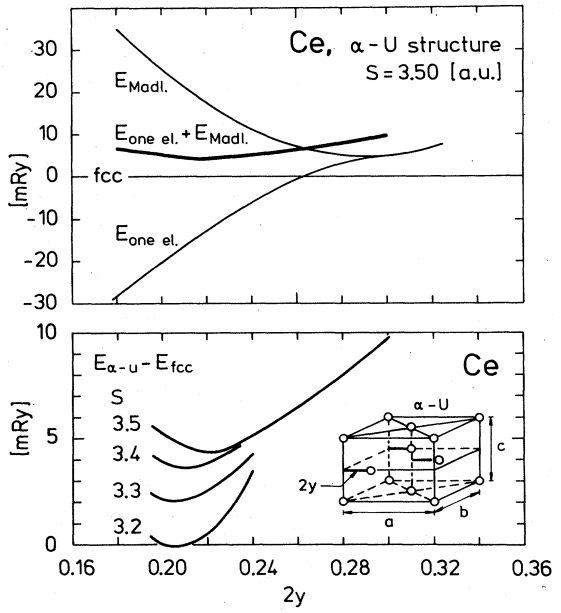

FIG. 16. Energy of Ce in the α-U structure, relative to the fcc phase, calculated as a function of the positional parameter $2y$ (see inset) and atomic radius s in a.u. The individual Madelung and one-electron contributions for one particular radius are shown in the upper panel.

of the unusual isostructural $\gamma \rightarrow \alpha$ transition. Here we shall be concerned with the fcc$\rightarrow\alpha$-U$\rightarrow$tetragonal crystal-structure sequence exhibited by metallic Ce at low temperature in the pressure range up to 20 GPa (see Fig. 15). In the calculations we shall treat the s, p, d, and $4f$ electrons on the same footing, i.e., as band electrons. Hence, we favor the picture of the $\gamma \rightarrow \alpha$ transition suggested by Gustafson *et al.*[94] and elaborated on by Johansson,[95] according to which pressure induces a Mott transition within the $4f$ shell such that the $4f$ electron goes from a localized state in γ-Ce to a delocalized, i.e., band state, in α-Ce.

According to the Mott-transition picture, Ce metal at pressures above the $\gamma \rightarrow \alpha$ transition is different from the other lanthanides (and indeed from all the other metals we have considered so far), in that it has a fourth conduction electron residing in the $4f$ band. It is this occupation of the $4f$ band which is expected to be responsible for the stability of the α-U structure found experimentally above 5.6 GPa,[96] and perhaps for the tetragonal phase found above 12.1 GPa.[97] To shed light on this question, we shall now present a series of calculations of structural stabilities for Ce under pressure, and compare the results with those obtained for La were the $4f$ band is essentially empty.

The orthorhombic α-U structure may be viewed as distorted fcc, where some of the face-centered atoms have been moved away from their positions, as described by the parameter $2y$, see Fig. 16. If $2y = 0.5a$ and $a = b = c$, one has the usual fcc unit cell. In the case of Ce the Madelung contribution to the structural energy favors a $2y$ of approximately 0.3 (see top panel of Fig. 16), but the one-electron contribution moves the minimum in the energy difference to $2y = 0.21$, which is the $2y$ value found experimentally in $_{92}$U.[60] Under pressure, the minimum is seen to move to slightly lower $2y$ values, and eventually the α-U structure becomes more stable than the fcc.

From Fig. 16 it is expected that Ce will exhibit a fcc$\rightarrow\alpha$-U phase transition at a pressure which is calculated to be 11.7 GPa. The experimental transition pressure is 5.6 GPa,[96] and the discrepancy may be attributed to the fact that the atomic-sphere approximation is less suited for open crystal structures such as the α-U structure. As may be seen in Fig. 16, the Madelung correction, which we could neglect for the close-packed crystal structures of the alkaline-earth and transition metals, is now of the same order of magnitude as the one-electron contribution. Hence, inadequacies in the Madelung approximation of the electrostatic contribution to the structural energy are magnified and lead to errors in the estimate of the stability of the α-U structure. A similar problem was recently encountered in the case of the open Cs IV structure in $_{55}$Cs metal.[41]

If we compare the structural energy differences for Ce and La (Figs. 14 and 16) under pressure, we find that while the α-U structure eventually becomes more stable than fcc in Ce, it does not do so in La. Since the $4f$ band is essentially unoccupied in La, whereas Ce has approximately one $4f$-band electron, the notion that f-band states are responsible for the stability of distorted crystal structures such as the α-U structure is strongly supported by the present calculations. It follows that the α-U structure would not become stable in Ce under pressure unless the $4f$ electrons were delocalized, i.e., bandlike, and therefore any adequate description of the α and α' phases in Ce must treat the $4f$ states on the same footing as the s, p, d states. In short, Ce is a $4f$-band metal.

The high-pressure tetragonal structure[97] of Ce may be

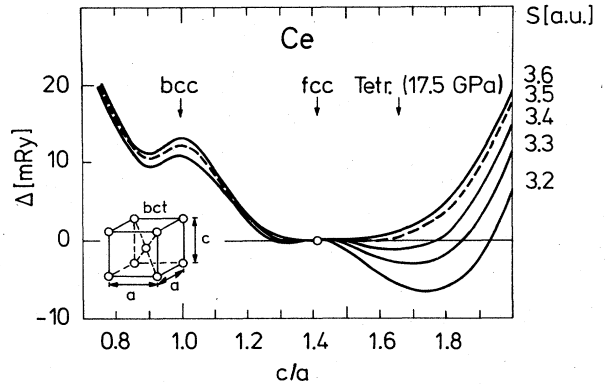

FIG. 17. Energy of Ce in the body-centered-tetragonal (bct) structure, relative to the fcc phase, calculated as a function of the c/a ratio and atomic radius (the pressures can be inferred from Fig. 18). The inset shows the bct structure.

regarded as a distorted fcc structure in which the unit cell has been elongated along the c axis such that the c/a ratio in a body-centered-tetragonal (bct) description is approximately 1.7; see Fig. 17. In the same description, bcc and fcc correspond to $c/a=1$ and $\sqrt{2}$, respectively. According to the structural energy differences in Fig. 17, Ce should, as a function of pressure, start out in the fcc structure and then transform into a bct structure with a c/a ratio which increases with pressure. In this case the $4f$ states do not seem to be responsible for the pressure-induced transition, since the same bct structure is also calculated to be the stable high-pressure phase of La, Fig. 14.

In Fig. 18 we have collected the calculated structural energy differences for Ce under pressure. Owing to the less accurate description of open structures discussed above, the α-U structure is seen not to be the stable phase in the pressure range considered, and, instead, Ce would be expected to go directly from the fcc into the bct phase. However, if we move the α-U curve down by 4.5 MRy (broken line in the figure), which is 20% of the Madelung correction (see Fig. 16), we obtain agreement with experiment[96,97] in the sense that Ce is now expected to exhibit the crystal-structure sequence fcc→α-U→tetragonal.

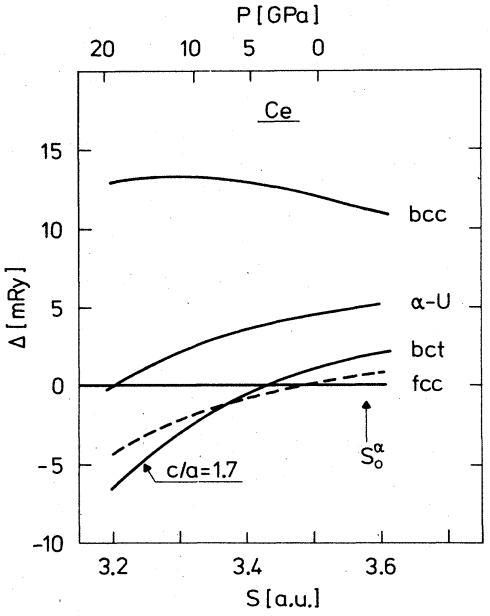

FIG. 18. Structural energy differences for Ce calculated as a function of pressure P and plotted vs atomic radius. S_0^α indicates the experimentally observed equilibrium radius of Ce in the α phase. The calculations included s, p, d, and f orbitals and the Madelung correction, Eq. (6).

G. The light actinide metals

The calculated structural energy differences for the light actinide metals $_{90}$Th—$_{94}$Pu are shown in Fig. 19, from which we deduce the most stable close-packed structure to be fcc in $_{90}$Th and $_{91}$Pa and bcc in $_{92}$U, $_{93}$Np, and $_{94}$Pu. This indicates that, although these structures are not the stable low-temperature structures in $_{91}$Pa—$_{94}$Pu, they are at least close in energy to the distorted structures observed experimentally, and may therefore be realized at elevated temperatures. Experimentally, one finds the fcc structure to be stable in $_{90}$Th up to 1670 K,[60] and there are indications that $_{91}$Pa has a high-temperature fcc phase.[60] Furthermore, neither $_{92}$U nor $_{93}$Np has a high-temperature fcc phase, but instead they become bcc before melting. $_{94}$Pu has a high-temperature fcc (δ) phase, but since this phase becomes unstable at a pressure of only 0.1 GPa it is most probably associated with a localization of the $5f$ electrons, and the relevant high-temperature phase in the present context is then the bcc (ϵ) phase. Thus, experimentally, the most stable close-packed structure appears to be fcc in $_{90}$Th and $_{91}$Pa, and bcc in $_{92}$U, $_{93}$Np, and $_{94}$Pu, in agreement with the findings in Fig. 19.

The low-temperature tetragonal structure (α) in Pa may be viewed[98] as a distorted bcc structure in which the unit

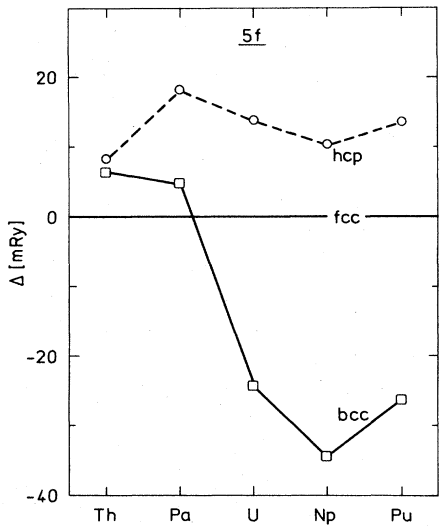

FIG. 19. Calculated structural energy differences for the light actinide metals plotted vs atomic number. The calculations included s, p, d, and f orbitals, but not the Madelung correction, Eq. (6).

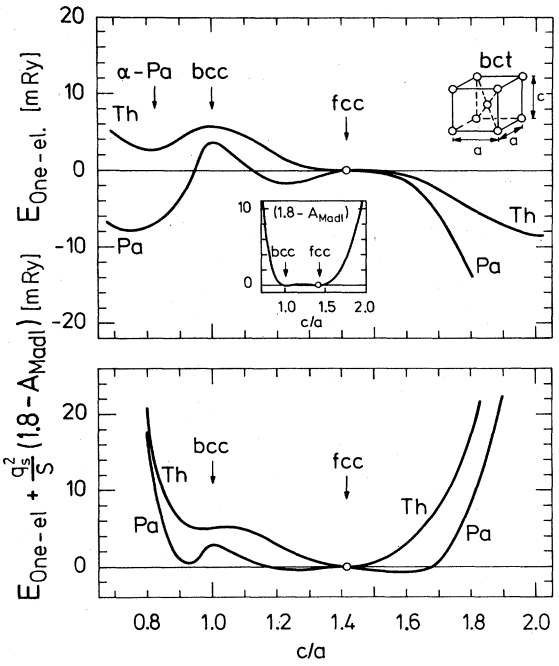

FIG. 20. Energy of Th and Pa in the bct structure, relative to the fcc phase, calculated as a function of the c/a ratio. The upper panel shows the one-electron contributions, the inset shows the shape of the Madelung correction, and the lower panel shows the total-energy differences.

cell has been compressed along the c axis such that the c/a ratio is approximately 0.82; see Fig. 20. According to Fig. 20 the Madelung contribution favors bct structures with c/a in the range 0.95—1.50, whereas structures with c/a outside this range rapidly become extremely unstable. In contrast, the one-electron contribution tends to favor c/a outside the central range, and, as a result, the energy-difference curve for Th has one minimum at $c/a=\sqrt{2}$, corresponding to fcc, in agreement with experiment, while that of Pa exhibits three minima, one of which is close to the c/a observed experimentally in the α phase.

As in the case of the α-U structure in Ce, we are again experiencing problems stemming from the atomic-sphere approximation and, in particular, the Madelung correction, which leads to slightly incorrect estimates of the structural energy differences for open crystal structures. Thus, in the case of Pa, the most stable structure is calculated to be bct with $c/a=1.6$, which incidentally is the high-pressure phase of Ce, whereas the minimum which corresponds to the experimental α structure lies 1.3 mRy above the absolute minimum and is shifted to a c/a of 0.92. However, in view of the rapidly changing Madelung correction in the range below $c/a=0.95$, it is not unlikely that a better calculation of the electrostatic contribution to the structural energy differences may correct both errors.

Since the $5f$ band is unoccupied in Th, while Pa has approximately one $5f$ electron, it follows from Fig. 20 that the $5f$ states are responsible for the stability of the tetragonal α phase in Pa. Thus, the situation here is very similar to that found earlier in Ce where the presence of one $4f$ electron stabilized the high-pressure α-U structure, and again we take this to mean that the $5f$ states in the light actinide metals are itinerant, i.e., bandlike, and give rise to distorted crystal structures.

VI. CONCLUSION

We have studied the stability of the crystal structures of some 40 elemental metals within a one-electron approach. The effective one-electron equations have been solved self-consistently by means of the LMTO method and the structural energy differences calculated by means of Andersen's force theorem. This approach has the advantage of treating s, p, d, and f states on the same footing, thus leading to a conceptually consistent description of trends throughout the Periodic Table. However, the present implementation of the method is only accurate for close-packed crystal structures, and for that reason we exclude in our study open structures such as Cs IV and the more exotic structures found in the actinide series. On the other hand, this shortcoming is not fundamental and will undoubtedly be remedied in the near future.

We find that the theory correctly predicts the crystal structures observed experimentally at low temperature and atmospheric pressure in 35 out of the 42 cases studied. In those few instances where the theory fails, we find that the correct crystal structure is only marginally less stable than the calculated structure—this is the case for $_{11}$Na, $_{79}$Au, $_{70}$Yb, and $_{91}$Pa—or that the metal is magnetic at low temperature, as in $_{25}$Mn, $_{26}$Fe, and $_{27}$Co. For the light actinide metals $_{92}$U, $_{93}$Np, and $_{94}$Pu we have not considered the experimentally most stable crystal structures, but only the most stable close-packed structures, and we find the predictions of the theory to be in qualitative agreement with the known phase diagrams.

In a comparison between the calculated structural energy differences for the $4d$ transition metals and the enthalpy differences derived from studies of phase diagrams, we find that, although the crystal structures are correctly predicted by the theory, the theoretical energy differences are up to a factor of 5 larger than their "experimental" counterparts. The reasons for this discrepancy may lie in the local-density approximation or in the neglect of the nonspherical part of the charge distribution. Furthermore, the derived enthalpy differences are certainly model dependent and may change as the model is improved.

In addition to the equilibrium properties, we have studied the crystal structures of the alkali, alkaline-earth, and some rare-earth metals under pressure. We find that the heavy alkali metals $_{19}$K, $_{37}$Rb, and $_{55}$Cs should be part of the crystal-structure sequence bcc→hcp→fcc where the intermediate hcp phase may be suppressed at room temperature, and explain the experimentally observed bcc→fcc transition in terms of the pressure-induced descent of a zone-boundary energy gap which exists in the fcc band structure but has no counterpart in the bcc case. For the alkaline-earth and rare-earth metals we find crystal-structure sequences which correlate with the calculated d-occupation numbers and which are in agreement

with experimental high-pressure observations if we neglect some complex structures found in $_{20}$Ca and $_{38}$Sr.

Finally, we have studied the high-pressure crystal-structure sequence fcc→α-U→tet for $_{57}$La and $_{58}$Ce. We find that under compression, the α-U structure becomes more stable than fcc in $_{58}$Ce, but not in $_{57}$La. This indicates that the presence of itinerant $4f$ states is responsible for the fcc→α-U transition observed experimentally in Ce. In both La and Ce the calculations predict a tetragonal high-pressure phase. This phase is seen experimentally in Ce, but not in La, where one observes, instead, a distorted fcc structure not considered in the present work.

In conclusion, we have studied the stability of crystal structures of metals both at equilibrium and at high pressures by a one-electron approach. We find that we can account for the occurrence of most of the close-packed structures observed experimentally. In the few cases where the theory is in disagreement with experiment, we find that the correct crystal structure is only marginally less stable than the predicted structure. In order to describe open structures, such as α-U or Cs IV, with the same accuracy as the close-packed structures, one needs a more accurate approximation for the electrostatic contribution to the total energy.

ACKNOWLEDGMENTS

The present series of calculations grew out of conversations with several people. It is thus a great pleasure to thank K. Syassen and K. Takemura for engendering my interest in the alkali-metal problem, and B. Johansson for suggesting the Ce problem. B. Johansson and A. K. McMahan have, furthermore, helped clarify calculational as well as experimental problems. A R. Mackintosh has kindly read the manuscript. Part of this work was started while visiting Los Alamos Scientific Laboratory, and I wish to thank the group at the Materials Science Center for its kind hospitality. Finally, the present work was supported by the Niels Bohr Foundation through the Royal Danish Academy of Sciences and Letters.

[1]L. Brewer, in *Batelle Institute Materials Science Colloquia,* edited by P. S. Rudman, J. Stringer, and R. I. Jaffee (McGraw-Hill, New York, 1967), pp. 39—67.
[2]L. Kaufman and H. Bernstein, *Computer Calculations of Phase Diagrams* (Academic, New York, 1970).
[3]R. A. Deegan, J. Phys. C 1, 763 (1968).
[4]N. W. Dalton and R. A. Deegan, J. Phys. C 2, 2369 (1969).
[5]F. Ducastelle and F. Cyrot-Lackmann, J. Phys. Chem. Solids **32**, 285 (1971).
[6]D. G. Pettifor, J. Phys. C 3, 367 (1970).
[7]D. G. Pettifor, in *Metallurgical Chemistry,* edited by O. Kubashewski (Her Majesty's Stationary Office, London, 1972).
[8]D. G. Pettifor, Comput. Coupling Phase Diagrams and Thermochem. (CALPHAD), **1**, 305 (1977).
[9]H. L. Skriver, Phys. Rev. Lett. **49**, 1768 (1982).
[10]B. Johansson and A. Rosengren, Phys. Rev. B **11**, 2836 (1975).
[11]See, for instance, B. J. Beaudry and K. A. Gschneidner, Jr., in *Handbook on the Physics and Chemistry of Rare Earths,* edited by K. A. Gschneidner, Jr. and L. R. Eyring (North-Holland, Amsterdam, 1978).
[12]A. Jayaraman and R. C. Sherwood, Phys. Rev. **134**, A691 (1964).
[13]G. J. Piermarini and C. E. Weir, Science **144**, 69 (1964).
[14]A. Jayaraman, Phys. Rev. **139**, A690 (1965).
[15]D. B. McWhan and A. L. Stevens, Phys. Rev. **139**, A682 (1965).
[16]D. B. McWhan and A. L. Stevens, Phys. Rev. **154**, 438 (1967).
[17]L.-G. Liu, W. A. Bassett, and M. S. Liu, Science **180**, 298 (1973).
[18]L.-G. Liu, J. Phys. Chem. Solids **36**, 31 (1975).
[19]A. Nakaue, J. Less-Common Met. **60**, 47 (1978).
[20]C. C. Koch, J. Less-Common Met. **22**, 149 (1970).
[21]W. A. Grosshans, Y. K. Vohra, and W. B. Holzapfel, Phys. Rev. Lett. **49**, 1572 (1982).
[22]Y. K. Vohra, H. Olijnyk, W. A. Grosshans, and W. B. Holzapfel, Phys. Rev. Lett. **47**, 1065 (1981).
[23]D. R. Stephens, H. D. Stromberg, and E. M. Lilley, J. Phys. Chem. Solids **29**, 815 (1968).
[24]J. Akella, Q. Johnson, W. Thayer, and R. N. Schock, J. Less-Common Met. **68**, 95 (1979).
[25]J. Akella, Q. Johnson, and R. N. Schock, Geophys. Res. **85**, 7056 (1980).
[26]R. B. Roof, R. G. Haire, D. Schiferl, L. A. Schwalbe, E. A. Kmetko, and J. L. Smith, Science **207**, 1353 (1980).
[27]R. B. Roof, Z. Kristallogr. **158**, 307 (1982).
[28]U. Benedict, J. R. Peterson, R. G. Haire, and C. Dufour, J. Phys. F **14**, L43 (1984).
[29]C. H. Hodges, Acta Metall. **15**, 1787 (1967).
[30]K. A. Gschneidner, Jr. and R. M. Valletta, Acta Metall. **16**, 477 (1968).
[31]J. C. Duthie and D. G. Pettifor, Phys. Rev. Lett. **38**, 564 (1977).
[32]B. Johansson, in *Rare Earths and Actinides, 1977,* edited by W. D. Corner and B. K. Tanner (IOP, Bristol, 1978), p. 39.
[33]A. R. Mackintosh and O. K. Andersen, in *Electrons at the Fermi Surface,* edited by M. Springford (Cambridge University Press, Cambridge, 1980).
[34]O. K. Andersen, H. L. Skriver, H. Nohl, and B. Johansson, Pure Appl. Chem. **52**, 93 (1979).
[35]For an illuminating argument, see V. Heine, in *Solid State Physics,* edited by H. Ehrenreich, F. Seitz, and D. Turnbull (Academic, New York, 1980), Vol. 35, p. 119.
[36]R. M. Nieminen and C. H. Hodges, J. Phys. F **6**, 573 (1976).
[37]D. G. Pettifor, Commun. Phys. **1**, 141 (1977).
[38]O. K. Andersen and O. Jepsen, Physica (Utrecht), **91B**, 317 (1977).
[39]J. A. Moriarty and A. K. McMahan, Phys. Rev. Lett. **48**, 809 (1982).
[40]A. K. McMahan and J. A. Moriarty, Phys. Rev. B **27**, 3235 (1983).
[41]A. K. McMahan, Phys. Rev. B **29**, 5982 (1984).
[42]A. O. E. Animalu, Phys. Rev. **161**, 445 (1967).
[43]V. Heine and D. Weaire, in *Solid State Physics,* edited by H. Ehrenreich, F. Seitz, and D. Turnbull (Academic, New York, 1970), Vol. 24.
[44]J. A. Moriarty, Phys. Rev. B **8**, 1338 (1973).
[45]J. A. Moriarty, Phys. Rev. B **26**, 1754 (1982).
[46]J. Hafner and V. Heine, J. Phys. F **13**, 2479 (1983), and refer-

ences therein.
[47]D. A. Young and M. Ross, Phys. Rev. B **29**, 682 (1984).
[48]A. Zunger and M. L. Cohen, Phys. Rev. B **18**, 5449 (1978); **20**, 4082 (1979).
[49]O. K. Andersen, Phys. Rev. B **12**, 3060 (1975).
[50]The zero-point energy is proportional to the Debye temperature, i.e., $E_0=\frac{9}{8}k_B\Theta_D$. Typically, Θ_D varies by 1—10 K between different structures of the same metal [see K. A. Gschneidner Jr., in *Solid State Physics,* edited by H. Ehrenreich, F. Seitz, and D. Turnbull (Academic, New York, 1964), Vol 16, p. 275] and hence the ΔE_0 to be added to (1) is of the order of 0.01—0.1 mRy which in most cases will be too small to affect the structural stabilities.
[51]W. Kohn and L. J. Sham, Phys. Rev. **140**, A1135 (1965).
[52]See, for instance, Ref. 54, Secs. 7.2 and 7.3, or Ref. 35, Secs. 13 and 15.
[53]U. von Barth and L. Hedin, J. Phys. C **5**, 1629 (1972).
[54]H. L. Skriver, *The LMTO Method* (Springer, Berlin, 1984).
[55]D. Glötzel and O. K. Andersen (unpublished).
[56]E. Esposito, A. E. Carlsson, D. D. Ling, H. Ehrenreich, and C. D. Gelatt, Jr., Philos. Mag. A **41**, 251 (1980).
[57]O. K. Andersen, J. Madsen, U. K. Poulsen, O. Jepsen, and J. Kollar, Physica (Utrecht), **86-88B**, 249 (1977).
[58]J. Friedel, in *The Physics of Metals 1. Electrons,* edited by J. M. Ziman (Cambridge University Press, Cambridge, 1969).
[59]H. L. Skriver, in *Systematics and the Properties of the Lanthanides,* edited by S. P. Sinha (Reidel, Dordrecht, The Netherlands, 1983).
[60]J. Donohue, *The Structures of the Elements* (Wiley, New York, 1975); D. A. Young, Lawrence Livermore Laboratory Report No. UCRL-51902, 1975 (unpublished).
[61]K. Takemura, S. Minomura, and O. Shimomura, in *Physics of Solids under High Pressure,* edited by J. S. Schilling and R. N. Shelton (North-Holland, Amsterdam, 1981).
[62]K. Takemura, S. Minomura, and O. Shimomura, Phys. Rev. Lett. **49**, 1772 (1982).
[63]K. Takemura, and K. Syassen, Phys. Rev. B **28**, 1193 (1983).
[64]H. Olijnyk and W. B. Holzapfel, Phys. Lett. **99A**, 381 (1983).
[65]B. Olinger, and J. W. Shaner, Science **219**, 1071 (1983).
[66]I. V. Alexandrov, C. V. Nesper, V. N. Katchinsky, and J. Marenko, paper presented at the 20th European High Pressure Research Group meeting, Stuttgart, 1982 (unpublished).
[67]K. Takemura and K. Syassen, Solid State Commun. **44**, 1161 (1982).
[68]H. T. Hall, L. Merril, and J. D. Barrett, Science **146**, 1297 (1964).
[69]J. Bardeen, J. Chem. Phys. **6**, 372 (1938).
[70]M. Born and J. E. Mayer, Z. Phys. **75**, 1 (1932).
[71]D. Glötzel and A. K. McMahan, Phys. Rev. B **20**, 3210 (1979).
[72]N. F. Mott and H. Jones, *The Theory of the Properties of Metals and Alloys* (Oxford University Press, London, 1936).
[73]H. Jones, Proc. Phys. Soc. **49**, 250 (1937).
[74]E. Bucher, P. H. Schmidt, A. Jayaraman, K. Andres, J. P. Maita, K. Nassau, and P. D. Dernier, Phys. Rev. B **2**, 3911 (1970).
[75]H. Olijnyk and W. B. Holzapfel, Phys. Lett. **100A**, 191 (1984).
[76]A. Jayaraman, N. Klement, Jr., and G. C. Kennedy, Phys. Rev. **132**, 1620 (1963).
[77]A. Jayaraman, Phys. Rev. **135**, A1056 (1964).
[78]A. Jayaraman, W. Klement, Jr., and G. C. Kennedy, Phys. Rev. Lett. **10**, 387 (1963).
[79]R. A. Stager and H. G. Drickamer, Phys. Rev. **131**, 2524 (1963).
[80]R. A. Stager and H. G. Drickamer, Science **139**, 1284 (1963).
[81]P. C. Souers and G. Jura, Science **140**, 481 (1963).
[82]D. B. McWhan, T. M. Rice, and P. H. Schmidt, Phys. Rev. **177**, 1063 (1969).
[83]J.-P. Jan and H. L. Skriver, J. Phys. F **11**, 805 (1981).
[84]K. J. Dunn and F. P. Bundy, Phys. Rev. B **24**, 1643 (1981).
[85]J. W. McCaffrey, J. R. Anderson, and D. A. Papaconstantopoulos, Phys. Rev. B **7**, 674 (1973).
[86]D. J. Mickish, A. B. Kunz, and S. T. Pantalides, Phys. Rev. B **10**, 1369 (1974).
[87]W. B. Holzapfel, T. G. Ramesh, and K. Syassen, J. Phys. (Paris) Colloq. **40**, C5-390 (1979).
[88]K. Takemura and K. Syassen, J. Phys. F (to be published).
[89]K. Syassen, G. Wortmann, J. Feldhaus, K. H. Frank, and G. Kaindl, Phys. Rev. B **26**, 4745 (1982).
[90]A. Rosengren and B. Johansson, Phys. Rev. B **13**, 1468 (1976).
[91]A. R. Williams (unpublished), and quoted in Ref. 92.
[92]A. R. Miedema and A. K. Niessen, Comput. Coupling Phase Diagrams and Thermochem. (CALPHAD) **7**, 27 (1983).
[93]L. G. Khvostantsev and N. A. Nikolaev, Phys. Status Solidi A **77**, 161 (1983).
[94]D. R. Gustafson, J. D. McNutt, and L. P. Roellig, Phys. Rev. **183**, 435 (1969).
[95]B. Johansson, Philos. Mag. **30**, 469 (1974).
[96]F. H. Ellinger and W. H. Zachariasen, Phys. Rev. Lett. **32**, 773 (1974).
[97]S. Endo, H. Sasaki, and T. Mitsui, J. Phys. Soc. Jpn. **42**, 882 (1977).
[98]H. Zachariasen, Acta. Crystallogr. **5**, 19 (1952).